

MIT Open Access Articles

Enhancing the surgeons reality : Smart visualization of bolus time of arrival and blood flow anomalies from time lapse series for safety and speed of

The MIT Faculty has made this article openly available. **Please share** how this access benefits you. Your story matters.

Citation: Copeland, A. et al. "Enhancing the surgeons reality : Smart visualization of bolus time of arrival and blood flow anomalies from time lapse series for safety and speed of cerebrovascular surgery." Applied Imagery Pattern Recognition Workshop (AIPRW), 2009 IEEE. 2009. 1-4. © Copyright 2009 IEEE

As Published: <http://dx.doi.org/10.1109/AIPR.2009.5466313>

Publisher: Institute of Electrical and Electronics Engineers

Persistent URL: <http://hdl.handle.net/1721.1/58955>

Version: Final published version: final published article, as it appeared in a journal, conference proceedings, or other formally published context

Terms of Use: Article is made available in accordance with the publisher's policy and may be subject to US copyright law. Please refer to the publisher's site for terms of use.



ENHANCING THE SURGEONS REALITY : SMART VISUALIZATION OF BOLUS TIME OF ARRIVAL AND BLOOD FLOW ANOMALIES FROM TIME LAPSE SERIES FOR SAFETY AND SPEED OF CEREBROVASCULAR SURGERY

Andrew Copeland^{1,2}, Rami Mangoubi¹, Mukund Desai¹, Sanjoy Mitter², and Adel Malek³

¹C.S. Draper Laboratory, Cambridge, Massachusetts

²Department of Electrical Engineering and Computer Science, MIT, Cambridge, MA

³Department of Neurosurgery, Tufts-New England Medical Center, Boston, MA

ABSTRACT

A noise adaptive Cusum-based algorithm for determining the arrival times of contrast at each spatial location in a 2D time sequence of angiographic images is presented. We employ a new group-wise registration algorithm to remove the effect of patient motions during the acquisition process. By using the registered image the proposed arrival time provides accurate results without relying on a priori knowledge of the shape of the time series at each location or even on the time series at each location having the same shape under translation.

1. INTRODUCTION

We present a new method for finding the arrival time of contrast at various points in the vasculature of the brain from a sequence of 2D X-ray angiograms. Determining the arrival times of the contrasts collapses the time series information down to a single image containing the arrival time at each pixel. The 2D arrival time information aids surgeons in assessing irregularities in the blood flows due to clots or other constriction. A surgeon would more easily observe delays in contrasts and quickly diagnose the presence of an anomaly.

As in [1] a method for the generation of “color coded images which indicate the arrival time of the contrast medium” is developed. Our approach uses an adaptive Cusum-based method [2] that provides a more accurate set of arrival times that does not rely on a priori knowledge of the shape of the time series at each location [1, 3, 4] or on the time series at each location having the same shape under translation [5]. The use of the Cusum algorithm is motivated by the wide variations in shape of the time series across different locations that due to the complicated interconnected network of blood vessels with a large range of diameters.

Before arrival times are determined, the effect of patient motions is removed from the time series by using a recursive groupwise registration algorithm that is applied to the 2D time series. A groupwise algorithm is used instead of pairwise

registration with the a single image because it allows vasculature, which is the focus of our study, to have an effect on the registration. This can be thought of as allowing features not present in all images to be weighed together. Once a feature is added to the representative image, the mean here, it can aid the registration of all images that contain it. Unlike most groupwise algorithms, such as in [6, 7], that process over the entire set of images at each step, the proposed algorithm consists of recursive application of pair wise registration between a representative image of an aligned set of images with the next image to be aligned.

2. METHODS

2.1. Groupwise registration

To compensate for patient motions in the 2D time series, a simple variation on the groupwise registration algorithms in [6, 7] is proposed that utilizes any pairwise registration algorithms [8, 9, 10, 11, 12] to produce a groupwise algorithm. The two image registration algorithm used here is presented in [11] and is based on a least squares difference criteria. The recursive algorithm begins on a set of images by first registering a pair of images with respect to one another and then finding a representative image of that pair. Subsequently, the next of the unregistered images in the set is registered with the representative image. Once registered, the image is added appropriately to the set of registered images and a new representative image is found. The process is repeated until each image is registered. In this study, the mean image is used as the representative image as in [13, 14]. In both [13] and [14] the mean is calculated over all images instead of the aligned set of images. Other choices for the representative image include the median image and the minimum entropy image.

An image in a time series from a single viewpoint is denoted $I_n[\mathbf{x}_p]$ at location $\mathbf{x}_p \in \mathbb{R}^2$ at time n . The term $I_n[\mathbf{x}_p]$ is interpreted as the bilinear interpolated value [15] of the image at the spatial coordinate \mathbf{x}_p . The terms \mathbf{T}_n and $\bar{\mathbf{T}}_n$ are defined as a coordinate transformation, and the best coordinate transformation, respectively, on the coordinates of image

Work supported by the C.S. Draper Laboratory, Cambridge Massachusetts.

n . In general, a wide variety of transformations is possible, both rigid and elastic. Here we follow [11] and use a globally rigid homogeneous transformation. The optimal transformation \bar{T}_n is given by

$$\bar{T}_n = \underset{T_n}{\operatorname{argmin}} \sum_{i=1}^L [I_n[T_n(\mathbf{x}_i)] - \mu_{n-1}[\mathbf{x}_i]]^2, \quad (1)$$

where L is the total number of pixels and $\mu_{i,n}$ is the mean of the first n images which is calculated recursively using

$$\mu_n[\mathbf{x}_i] = \frac{(n-1)\mu_{n-1}[\mathbf{x}_i] + I_n[T_n(\mathbf{x}_i)]}{n}. \quad (2)$$

2.2. Determining arrival times

Overview: A general method that looks for large changes in the intensity at each pixel location due to the presence of contrast is desired for determining the arrival time of contrast at each point in the 2D time series. An adaptive variation of the Cusum algorithm [16] can accomplish this. The Cusum algorithm can be interpreted as a special application of the repeated Sequential Probability Ratio Test or SPRT such as in [17]. The Cusum algorithm works by thresholding an indicator function $h_n[\mathbf{x}_i]$

$$h_n[\mathbf{x}_i] = \left[h_{n-1}[\mathbf{x}_i] - \frac{I_n[\bar{T}_n(\mathbf{x}_i)] - \mu_{n-1}[\mathbf{x}_i]}{q(\mu_{n-1}[\mathbf{x}_i])} - \tau \right]^+, \quad (3)$$

where $\mu_n[\mathbf{x}_i]$ is as defined in Equation 2, τ is a threshold, $h_0[\mathbf{x}_i]$ is zero, $[\cdot]^+ = \max(\cdot, 0)$, and q a function representing the noise level at a point. This intensity-based noise level makes the overall algorithm adaptive as does the application of an adaptive worst case error term to the repeated SPRT test in [18]. Another approach to adaptation is presented in [19]. The expression inside the one-sided test is simply the previous indicator function plus the number of standard deviations the current image at location \mathbf{x}_i is below the cumulative mean $\mu_{n-1}[\mathbf{x}_i]$ less a threshold τ . In order to remove outliers during the generation of the indicator function, a median filter [15, 20] is applied to the image defined by the fraction in Equation 3 at each time.

Estimating noise level: As is typical with CCD images, the X-ray noise level depends on the intensity of the detected value [21]. The affine model

$$q(v) = v \cdot a + b, \quad (4)$$

where v is a scalar intensity is used here.

The first step, calculating the coefficients a and b , is accomplished by calculating noise levels in the image. This is done by generating the joint histogram between the first two registered images. These images are chosen so that the image changes are due to the noise in the image acquisition, not the presence of contrast or of patient motions. From the

joint histogram we are able to determine the conditional PDF $P_{I_2|I_1}(I_2[\bar{T}_2(\mathbf{x}_i)] = v_2 | I_1[\bar{T}_1(\mathbf{x}_i)] = v_1)$. From the conditional probabilities we can determine the conditional standard deviation $\sigma(I_2|I_1 = v_1)$ for each v_1 which will be denoted by the shorthand $\sigma(v_1)$. We then perform a least square affine fit to find the best estimator of $\sigma(v_1)$, $q(v_1) = a * v_1 + b$. This is done by using a weighting on the variance of each term based on the total number of image points with a particular intensity. This minimization is equivalent to

$$\{a, b\} = \underset{a, b}{\operatorname{argmin}} \sum_{v_1 \in \operatorname{Range}(I_1)} (\sigma(v_1) - av_1 - b)^2 P_{I_1}(v_1). \quad (5)$$

Determining arrival times: After the indicator function is generated, it is thresholded to detect abrupt changes, or when the contrast is first detected. Using a high threshold rejects many false alarms, but it also makes it difficult to detect when the contrast first arrives. Once the contrast is detected, the algorithm steps back in time until it reaches the time immediately after it crossed a second lower threshold. The time the intensity goes above the second threshold is the arrival time we assign to that point in the 2D image.

The Cusum algorithm detects an abrupt change at time n_f when h_{n_f} first exceeds the threshold τ_f . We determine the arrival time n_a contrast to be

$$n_a = \underset{n \in [1, n_f - 1]}{\operatorname{argmax}} h_{n-1} < \tau_a, \quad (6)$$

for some threshold τ_a . This final step results in the 2D collection of arrival times $n_a[\mathbf{x}_i]$.

3. RESULTS

3.1. Registration

The results of applying the groupwise algorithm to a series of image is presented in Figure 1, where a depiction of the error in a stack of images before and after registration is shown. The reduction in the error in the bone in the upper left corner

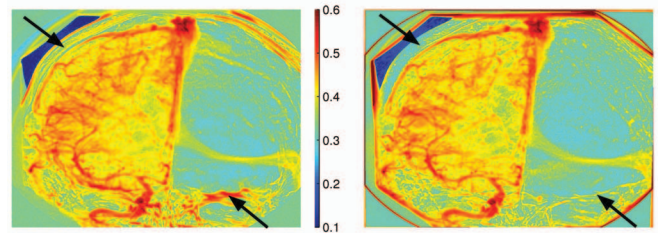


Fig. 1. RMSE Visualization – The figure shows a contrast enhanced image of the RMSE of each pixel across all of the images for the unregistered (left) and registered series (right). The numerical performance of the algorithm is shown in Table 1.

and the area around the eye sockets is pronounced (see arrows). The high RMSE in locations where contrast is present

Method	Total RMSE		
	No Reg.	Reg. vs Frame 1	Groupwise
Total	0.0213	0.0215 (-1%)	0.0193 (9%)
Unchanged	0.0181	0.0186 (-3%)	0.0112 (38%)

Table 1. The RMSE of the of the total error, or ε , between each pair of the 16 images. The two rows show results based on the whole image (1st row) and all regions without contrast (2nd row). The methods used: no registration (baseline), pairwise registration to first image, groupwise algorithm.

is due to the varying intensity as contrast flows in and out. In the sequence of images there is a mask with a fixed location that is used in the X-ray process. When registering the foreground, the head, the background, the mask, is moved causing errors in the boundary between the two. Table 1 shows the numerical improvement in the root mean square error (RMSE) of a stack of images. Also note that on the regions that the contrast does not impact pixel intensity (Unchanged Area) the forward groupwise algorithms produce up to 38% percent reduction in the RMSE. Although the error is reduced, artifacts remain that can be attributed to out of plane patient rotations.

3.2. Arrival Times

Using the noise measurements based on Equations 4 and 5, Figure 2 shows the arrival time estimates for a different sequence of 105 images where contrast was injected into the vertebral artery. The results shown are for the threshold choices of τ , τ_f , and τ_a shown in the captions; they can be tuned to increase the sensitivity or to avoid assigning arrival times for locations where no contrast appears.

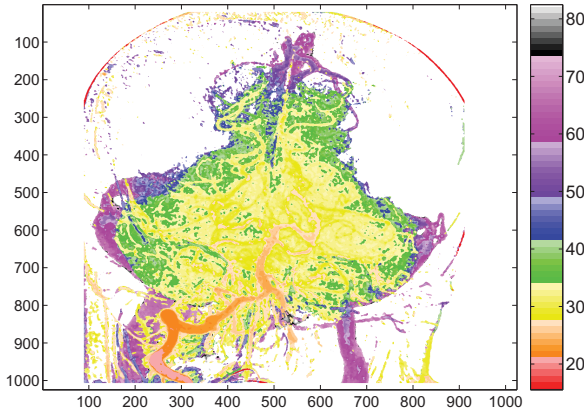


Fig. 2. 2D Arrival Times – Arrival times measured by the Cusum algorithm. Contrast was injected into the vertebral artery. For this figure $\tau_f = 2$, $\tau_a = 0.1$, and $\tau = 1$. The color bar is used to show the arrival time (frames) of the contrast.

Figure 3(a) plots the time series for four separate locations (the blue and green lines are for locations with a pronounced response, while the cyan and red lines are for loca-

tions with a more subtle response). The recursively calculated mean in Equation 3 is depicted with a dotted line. The blue and green time series are clearly not simply shifted and scaled versions of one another, which suggests that the proposed Cusum method is more appropriate. If the image values drop below the dotted line, the indicator function in Equation 3 will be non-zero as shown in Figure 3(b). When this drop normalized by the adaptive variance is larger than the threshold the indicator function at that time will increase. In Figure 3(b) the indicator function for the blue and green time series crosses the two thresholds more quickly than the function for the cyan and red plots. This is due to the smaller change in the image intensities. We expect the algorithm to be less accurate on less pronounced weaker signals.

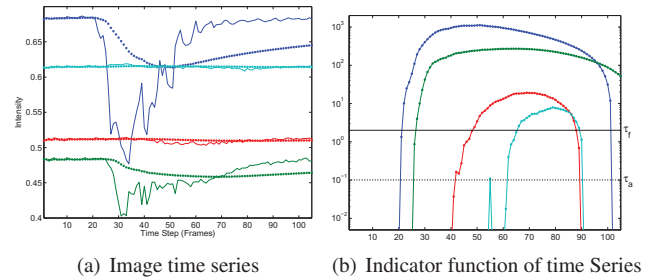


Fig. 3. Time Series and Indicator function. The blue, green, cyan, and red lines are from data located at the points (934, 253), (620, 578), (460, 300), and (155, 454) in Figure 2 respectively. Intensity plots are shown in the left panel for the 4 locations. A dotted line for each plot shows the recursively calculated mean used in Equation 2. The indicator function (see Equation 3) for the four locations are shown in the right panel. The solid and dotted black lines show the location of thresholds τ_f and τ_a , respectively.

The arrival time algorithm finds the contrast arrival times for the blue and the green time series are 21 and 26 respectively, which we verified by visual inspection. However, modifying the algorithm in [5] so that the first and lowest values of the blue time series are the same as that of the green series yields a result of relative shift of 25 frames which can be compared to the relative shift of 5 frames by our algorithm. This difference is due to the green time series taking longer to return to normal than the blue time series. This result illustrates that the Cusum-based method, which makes no assumption about the waveform, is appropriate for this application.

Figure 4 shows a zoomed in version of the arrival times for both of the Cusum and for the correlation methods. The regions tend to be well defined although there are clearly some areas where the estimates of the contrast arrival times are out of order. The results for the Cusum shows fewer breaks along the blood vessels. In addition the correlation method picked up arrival times consistent with the exit of contrast, as opposed to the arrival, from the brain. This takes place because the size of the vessels for blood entering the brain are smaller than those for blood exiting the brain. The signal for the blood exiting the brain is stronger at these location thereby causing

the correlation algorithm to break down.

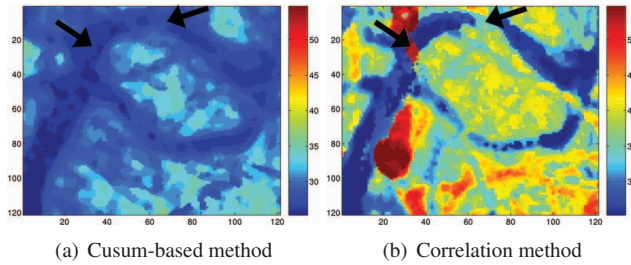


Fig. 4. Zoomed in View of 2D Arrival Times – Zoomed in View of Arrival times for set of images used in Figure 2 for both the Cusum and the correlation methods. The two arrows show two of the regions where there is a break in the arrival times within a part of the blood vessel. The left arrow shows a break that appears only in the correlation plot, where times were assigned to a stronger signal for contrast exiting the brain. The right arrow shows a less drastic difference where the arrival times in the gap were off by 8 frames from the vessel as opposed to 3 frames.

4. CONCLUSION

The new noise adaptive Cusum-based algorithm provides a more accurate measurement of the 2D times of arrival. This method does not depend on the shapes of the time series. In addition, the registration algorithm reduced the effect of the patients motion, however several artifacts can remain due to motion from out of plane rotations.

Assuming the observation time is long enough to flush contrast from the head, the arrival time algorithm can be run in reverse to determine the exit time of the contrast. This practice would highlight structures where the contrast leaves the brain. These structures are often occluded by other structures at the same location within the X-ray where contrast arrived at an earlier time. This algorithm provides surgeons a more accurate visualization for use during procedures.

5. REFERENCES

- [1] I. Horiba, A. Iwata, N. Suzumura, Y. Yamagishi, Y. Miyagi, T. Uwatoko, and Y. Mizuno, "Blood flow phase detection on digital subtraction angiography," in *Acoustics, Speech, and Signal Processing, IEEE International Conference on ICASSP '86*, vol. 11, Tokyo, 1986, pp. 1757–1760.
- [2] A. Wald, *Sequential Analysis*. New York: Wiley, 1947.
- [3] A. Santos, S. Furuie, and M. Gutierrez, "Estimation of coronary blood flow by contrast propagation using simulated x-ray angiography," in *Computers in Cardiology 1999*, Hannover, Germany, 09/26/1999 - 09/29/1999 1999.
- [4] Z. Wu and J.-Z. Qian, "Real-time tracking of contrast bolus propagation in x-ray peripheral angiography," in *WBIA '98: Proceedings of the IEEE Workshop on Biomedical Image Analysis*. Washington, DC, USA: IEEE Computer Society, 1998, p. 164.
- [5] H. Schmitt, M. Grass, V. Rasche, O. Schramm, S. Hähnel, and K. Sartor, "An x-ray based method for the determination of the contrast agent propagation in 3d vessel structures," *IEEE Trans. Med. Imaging*, vol. 21, no. 3, pp. 251–262, 2002.
- [6] E. G. Miller, "Learning from one example in machine vision by sharing probability densities," Ph.D. dissertation, M.I.T., February 2002.
- [7] A. Tsai, J. Anthony Yezzi, W. Wells III, C. Tempany, D. Tucker, A. Fan, W. E. Grimson, and A. Willsky, "Model based curve evolution technique for image segmentation," *IEEE Computer Society Conference on Computer Vision and Pattern Recognition*, vol. 1, pp. 463–468, 2001.
- [8] P. A. Viola, "Alignment by maximization of mutual information," Ph.D. dissertation, M.I.T., June 1995.
- [9] B. Horn and B. Schunck, "Determining optical flow," *Artificial Intelligence*, vol. 17, pp. 185–203, 1981.
- [10] Q. Tian and M. N. Huhns, "Algorithms for subpixel registration," *CVGIP*, 1986.
- [11] S. Zokai and G. Wolberg, "Image registration using log-polar mappings for recovery of large-scale similarity and projective transformations," *IEEE Transactions on Image Processing*, vol. 14, no. 10, pp. 1422–1434, October 2005.
- [12] R. Bajcsy and S. Kovacic, "Multiresolution elastic matching," *Vis., Graph., Image Process.*, vol. 46, pp. 1–21, 1989.
- [13] B. Davis, P. Lorenzen, and S. Joshi, "Large deformation minimum mean squared error template estimation for computational anatomy," in *Proceedings of the IEEE International Symposium on Biomedical Imaging*, April 2004, pp. 173–176.
- [14] C. Twining, S. Marshland, and C. J. Taylor, "Groupwise non-rigid registration: The minimum description length approach," in *Proceedings of the British Machine Vision Conference*, vol. 1, 2004, pp. 417–426.
- [15] J. S. Lim, *Two-Dimensional Signal and Image Processing*. Prentice Hall PTR, 1999.
- [16] M. Basseville and I. Nikiforov, "Detection of abrupt changes: theory and application," 1993.
- [17] A. Shiryaev, "The problem of the most rapid detection of a disturbance in a stationary process," *Soviet Math. Dokl.*, no. 2, pp. 795–799, 1961.
- [18] M. N. Desai, J. C. Deckert, and J. J. D. Jr., "Dual-sensor failure identification using analytic redundancy," *Journal Guidance and Control*, vol. 2, no. 3, pp. 213–220, May-June 1979.
- [19] T.-T. Chen and M. Adams, "A sequential failure detection technique and its application," *IEEE Transactions on Automatic Control*, vol. 21, no. 5, pp. 750–757, October 1976.
- [20] E. Ritenour, T. Nelson, and U. Raff, "Applications of the median filter to digital radiographic images," in *Acoustics, Speech, and Signal Processing, IEEE International Conference on ICASSP '84*, vol. 9, March 1984, pp. 251–254.
- [21] G. E. Healey and R. Kondepudy, "Radiometric ccd camera calibration and noise estimation," *IEEE Transactions on Pattern Analysis and Machine Intelligence*, vol. 16, no. 3, pp. 267–276, March 1994.